Methane combustion over copper chromite catalysts

Giovanni Comino, Antonella Gervasini* and Vittorio Ragaini

Dipartimento di Chimica Fisica ed Elettrochimica, Università degli Studi di Milano, via C. Golgi 19, I-20133 Milan, Italy

Zinfer R. Ismagilov

Boreskov Institute of Catalysis, Department of Environmental Catalysis, Pr. Ak. Lavrentieva 5, Novosibirsk 630090, Russia

Received 25 May 1997; accepted 14 August 1997

A study of the activity and durability of two different copper chromite catalysts in methane combustion is presented. The catalysts, a massive (CAT-E) and a supported (CAT-I) copper chromite, were characterized by different techniques in order to investigate morphological properties (N_2 adsorption), crystalline structure (X-ray diffraction, XRD) and surface composition (X-ray photoelectron spectroscopy, XPS). Among the different crystalline phases identified, $CuCr_2O_4$ spinel represented the common phase in both the catalysts. The Cr^{VI}/Cr^{III} surface ratio was almost the same for the two catalysts, while the Cu^{II}/Cu^{I} surface ratio was much higher on the massive catalyst than on the supported one. The activity for CH_4 combustion was studied in the temperature range 300–700°C at constant CH_4 : air ratio of 1 : 30 and constant methane content, 1.2%. The activity was higher for CAT-I and CAT-E showed better stability. A kinetic study from the catalytic data, collected at different contact times in the interval 0.047–0.315 s as a function of temperature, provided a value of about 110 kJ/mol for the activation energy. This value was obtained for various degrees of methane converted for the two catalysts. The reaction rates were between 10^{-3} and 10^{-4} $(mol_{CH_4})_{conv}/(g\,h)$ in the temperature interval 550–700°C, for both the catalysts.

Keywords: copper chromite, methane, oxidation, catalyst characterization, kinetic analysis

1. Introduction

In the last few years new extremely stringent standards in emission legislation have required the development of new technologies for both clean energy production and emission control, either for industrial or for household appliances.

Among the processes of energy production, high temperature combustion of fossil fuels is the most conventionally used [1–4]. During combustion, the formation of pollutants, in particular NO_x, is favored due to the high temperatures attained [1,2,5].

Catalysis can offer the possibility to realize clean combustion in an interval of temperature in which the formation of given pollutants, e.g. NO_x, is depressed [1–4,6,7]. The choice of the appropriate catalyst is a fundamental step for improving the combustion, in terms of both activity and selectivity, limiting the formation of hazardous by-products [1,3].

Various materials have found applications as active components for catalytic combustion appliances [8–10]. The correspondence between the rate of hydrocarbon oxidation and the metal–oxygen bond strength represents a well known general criterion for the choice of the active component of a combustion catalyst [4,9]. This correlation leads to a volcano shape curve and a clear maximum for platinum-group metals is observed. The high activity of noble metals is due to their capability to activate O_2, H_2 and C–H and O–H bonds on their surface [1,2,10]. Generally, metal catalysts are prepared depositing the metal on ceramic oxide supports to improve metal dispersion and thermal stability. The performances of Pt or Pd with respect to hydrocarbons combustion, in particular methane, have been largely studied by many authors [11–17]. Burch et al. [11] have reported that Pt-catalysts have higher activity at low $O_2 : CH_4$ ratio while Pd-catalysts are more active in oxygen rich conditions.

The use of noble metals has stringent effects on the commercial cost of the whole catalyst, so that a great interest has turned to oxide-based catalysts [18–22]. Recent developments in the field of oxide-type catalysts deal with perovskites structures [18–20]. Arai et al. [18], have found that $LaCoO_3$, $LaMnO_3$ and $LaFeO_3$ exhibit activity for methane combustion similar to that of Pt-catalysts. However, temperatures over 600°C are responsible of an activity decay of the perovskites structure [18]. Hexa-aluminated structures have also been utilized in combustion reactions [3,19,20]. Their main advantage is the high and stable value of surface area at very high temperatures (> 1200°C), nevertheless they show a lower activity than noble metals and perovskites catalysts.

Among conventional oxide-based systems, transition metal oxides present lower activity and require higher light-off temperatures than the metal catalysts [9] but generally they have higher stability in work conditions (i.e., high temperature and presence of water) [1,3,9].

* To whom correspondence should be addressed.

Simple metal oxides containing elements that can undergo redox cycles varying their valence state are the most interesting ones. Among these, the elements Cr, Co, Ni, and Mn show a promising behaviour: in particular good activity of Co_3O_4 and Cr_2O_3 is reported [1]. Mixed oxide compositions show better activity than the single oxide ones [1,9]. Due to the good stability of their structure, they could offer interesting performances in combustion reactions. Prasad et al. [23], utilized oxides of Cr and Co deposited on alumina wash-coated honeycomb for the combustion of propane, modelling the global mechanism composed of three first-order reactions.

In this work two different mixed transition metal oxides have been studied for methane complete oxidation. The catalysts were a massive copper chromite (CuO–Cr_2O_3) and an alumina-supported one (CuO–Cr_2O_3/γ-Al_2O_3). The former has been already successfully used in the complete oxidation of volatile organic compounds and it was also comparatively tested with noble metal catalysts [24,25]. First, the physical and chemical properties of both catalysts were determined, second, their activity in terms of methane conversion was compared. The stability of the two catalysts was investigated by means of discontinuous combustion tests performed in a significant region of methane conversion (20–90%). Moreover, a kinetic study was performed in order to calculate activation parameters.

2. Experimental

2.1. Catalyst

Two different copper-chromite-based catalysts were studied towards complete methane combustion. The first catalyst, designated as CAT-E (E-1230, from Engelhard), was a massive copper chromite catalyst in which alumina was present as a binder (ca. 30 wt%). The second catalyst, designated as CAT-I, was a supported copper chromite catalyst (ca. 60 wt% of Al_2O_3) prepared by conventional impregnation technique from nitrate salt precursors and eventually calcined at 600°C for 4 h.

The two catalysts were characterized by means of ionization coupled plasma (ICP), X-ray photoelectron spectroscopy (XPS), X-ray diffraction (XRD), and N_2 adsorption techniques to determine chemical and surface composition, crystalline structure and surface area and pore size distribution, respectively.

Before use, both catalysts were crushed and sieved to obtain particle size between 500 and 710 μm, they were eventually calcined at 700°C for 5 h.

2.2. Catalyst characterization

The composition of both catalysts was determined by conventional ICP analysis using a JY24 Jobin Yvon instrument. A small quantity of catalyst powder (10 mg) was treated with HNO_3 and HF, brought to the boil for a few minutes and then treated with $HClO_4$ in order to completely oxidize fluorine ions to F_2 to avoid interference during the analysis. The solution was diluted with distilled water and then analyzed. This procedure gave unreliable results for CAT-I because of the higher alumina content. Then, the nitric solution of CAT-I was subjected to a sonication treatment to obtain complete solubilization.

The principal elements contained in both the catalysts were Al, Ba, Cr and Cu and they were quantitatively determined at 394.401, 455.403, 205.552, and 324.754 nm, respectively. Table 1 reports the chemical composition and the Cu/Cr molar ratio of the catalysts.

The specific surface area, pore volume and pore distribution as a function of their radius were determined by N_2 adsorption isotherms. The analysis was performed by a Sorptomatic 1900 (Fisons Instruments) equipped with the Milestone 200 acquisition program. Surface area was calculated from the BET equation and pore distribution from Horvath–Kawazoe model [26]. The dependence of specific surface area on temperature was investigated performing thermal treatments of fresh portions of the catalysts in air in the temperature range 400–1000°C for 5 h.

XRD analysis, performed by a D/max-C Rigaku instrument (Cu Kα radiation, $\lambda = 1.54178$ Å), was used to identify the crystalline phases of the two catalysts.

The surface elemental composition and the oxidation state of the identified elements were determined by XPS analysis using a Surface Science Instruments M-Probe. The source provided a monochromatic Al Kα radiation (1486.60 eV). The pressure in the analysis chamber was typically 5×10^{-9} mbar. A spot size of 400×1000 μm and a pass energy of 150 eV were used for survey spectra, while for the single-region acquisitions a spot size of 200×750 μm and a pass energy of 25 eV were used. All XPS peaks were fitted using a peak-fitting routine. The lines used in fitting a peak envelope were defined according to their centered position, half-width, shape (a combination of Gaussian and Lorentzian distributions) and intensity. The best fit of the experimental curve was searched by a tentative combination of bands.

2.3. Catalyst testing

Catalysts were tested in a laboratory flow reactor system operating at atmospheric pressure. The catalyst (1

Table 1
Catalyst composition

Catalyst	Composition (wt%)				Cu/Cr molar ratio
	Cr	Cu	Al	Ba	
CAT-E	14.8	22.1	15.0	5.1	1.22
CAT-I	7.7	9.0	26.4	2.1	0.95

cm^3), supported by a quartz bed, was placed centrally in a stainless steel reactor (AISI 316, 26 mm i.d., 20 cm long). A thermocouple was placed in the centre of the catalyst bed to monitor the temperature. The reactor was mounted in a vertical tube furnace heated by a temperature controller (from Ascon, XS series). The temperature of the furnace was monitored using a chromel–alumel thermocouple situated on the wall at the mid point of the furnace.

The feed gases were methane (from SIAD, 99.995% purity), air and nitrogen (from Tecnogas, 99.999% purity). Their streams were regulated and controlled by mass flow meters (from Bronkhorst, EL series). The total flow of the feed was varied from 76.4 to 11.4 Nℓ/h in order to realize contact times (τ) in the interval 0.047–0.315 s (τ expressed in $(cm^3)_{cat}/(cm^3/s)_{flow}$). All the catalytic runs were carried out at constant partial pressure of CH_4 ($p_{CH_4} = 0.012$ atm) and constant CH_4 : air ratio of 1 : 30.

During a typical run, first the catalyst was heated at 550°C for 4 h in air at the same flow successively used in the combustion test (11.4–76.4 Nℓ/h). Second, the temperature was lowered to 300°C in air flow. During cooling, the reaction mixture was analyzed through an auxiliary line to determine the CH_4 concentration of the feed. The combustion tests were carried out in the temperature range from 300 to 700°C increasing the temperature by steps of 50°C. Each heating step was performed in air, at the attainment of the steady value of temperature, the reaction mixture was re-introduced in the reactor.

The feed and the product gases were analyzed by a TOC (total organic carbon) apparatus from N.I.R.A. Instruments (801-F). The sample gas was taken by a sampling valve into a loop (2 cm^3) maintained at 80°C. First, it was taken to atmospheric pressure and then it was sent to the detector system (flame ionization detector, FID). Each analytical datum presented corresponded to an average of 60 values collected at intervals of 30 s during 30 min of acquisition routine. Calibration measurements were carried out with a CH_4 : air mixture having known methane concentration of 512 ppmV.

Activity of catalysts was defined as the percent conversion of CH_4, that is $[(ppm(CH_4)_{in} - ppm(CH_4)_{out})/ppm(CH_4)_{in}] \times 100$.

3. Results and discussion

3.1. Catalyst characterization

The two catalysts had the same qualitative elemental composition but they differed in the amount of the different elements (table 1). The massive copper chromite, CAT-E, had a higher content of Cr and Cu than CAT-I, the supported one. The Cu/Cr molar ratio was, however, very close for the two catalysts. The difference in aluminum content characterized the supported from the massive catalyst (26.4 and 15.0 wt% of Al for CAT-I and CAT-E, respectively).

The morphological properties of both the catalysts were studied by N_2 adsorption in order to determine the specific surface area, pore volume and pore size distribution as a function of temperature. Sintering and phase collapse phenomena, responsible of surface area lowering, could be effective at the high temperatures attained during methane combustion. Figure 1 reports the results obtained from N_2 adsorption in terms of values of specific surface area as a function of temperature, for CAT-E and CAT-I. Surface area of CAT-E decreased from 106 to 35 m^2/g as temperature increased from 400 to 1000°C. Surface area of CAT-I was not strongly dependent on temperature, as revealed by the slight slope of the line reported in figure 1. In fact, starting from a value of 63.85 m^2/g of fresh CAT-I (600°C), a value of 57.07 m^2/g was found for treatment at 700°C. The porosity of the two catalysts was in the mesopore region. A decrease of about 40% of the total pore volume was observed for CAT-E for treatment at high temperature (0.600 cm^3/g at 400°C and 0.386 cm^3/g at 700°C), while the total pore volume of CAT-I was quite independent of temperature (0.198 and 0.162 cm^3/g at 600 and 700°C, respectively). The average pore radius varied from 63 to 80 Å as temperature increased from 400 to 700°C for CAT-E, while the average pore radius of CAT-I decreased from 52 to 46 Å in the same temperature interval. For CAT-I, the decrease of average pore radius with temperature is due to alumina presence, while the increase of average pore radius observed for CAT-E is indicative of modification of the morphology of the active phases of the massive copper chromite.

The crystalline structure of the two samples was studied by XRD analysis, the crystalline phases identified are presented in table 2. Both catalysts showed the

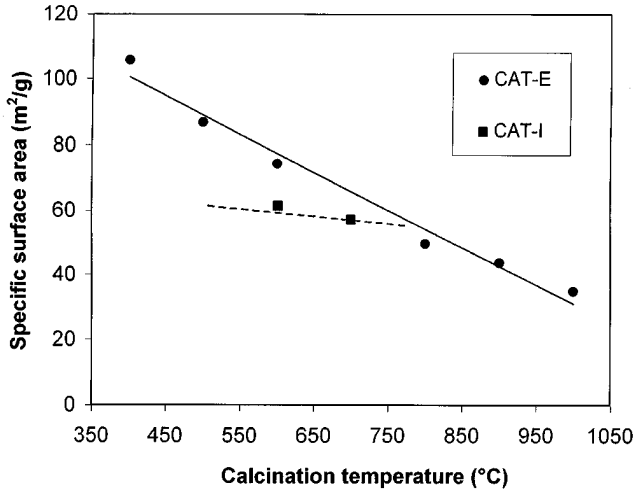

Figure 1. Dependence of surface area on calcination temperature for CAT-E and CAT-I.

Table 2
Identified crystalline phases of the catalysts by XRD analysis

Catalyst	Crystalline phase
CAT-E	**$CuCr_2O_4$**, $BaCrO_4$, $BaCr_2O_4$, Cu_4O_3
CAT-I	**$CuCr_2O_4$**, $CuCrO_4$, $Cu_2Cr_2O_4$, CuO, Cu_2O

$CuCr_2O_4$ spinel as common phase. Chromium containing single oxidic phases were never observed in both the samples. Two main phases characterized CAT-E: $BaCrO_4$/$BaCr_2O_4$ and $CuCr_2O_4$; $CuCrO_4$ and $CuCr_2O_4$ were the main phases of CAT-I. The massive copper chromite showed a more crystalline character than the supported one, which was quite amorphous according with its higher alumina content.

The surface elemental composition of the catalysts was determined by XPS analysis. Table 3 reports the results obtained as atomic percent of the elements present on the surface, their binding energy and oxidation state. Atomic ratios of the redox couples of the active elements (Cr and Cu) are also reported in table 3. It was revealed that total surface chromium content on CAT-E was about three times higher than on CAT-I. Ba and Cu were present on the surface in almost the same amount in both the catalysts (ca. 0.5% for Ba and 2.6% for Cu, table 3). It can also be seen that Al was only found on CAT-I surface, while it was absent on CAT-E surface, as expected due to the role of binder of alumina in the massive catalyst. As concerns the surface atomic ratio of the red-ox couples of Cr and Cu, it was revealed that the Cr^{VI}/Cr^{III} ratio was quite similar for the two samples, while a deep difference was observed for the Cu^{II}/Cu^{I} couple. The Cu^{II}/Cu^{I} ratio on CAT-E surface was more than eight times higher than that found on CAT-I (table 3).

3.2. Catalyst activity and durability

The catalytic activity of the two catalysts was studied for complete oxidation of methane in a flow reactor according to the operating procedure reported in the experimental section. Figures 2 and 3 report the CH_4 conversion as a function of reaction temperature at a contact time of 0.15 s for both the catalysts. The first run of the catalytic tests, collected on fresh catalysts, revealed that the massive catalyst (CAT-E) showed a higher light-off temperature than CAT-I. At each reaction temperature, CAT-I was more active than CAT-E. The difference in the combustion activity between the two catalysts could not be ascribed to morphological factors, i.e. different surface areas between CAT-I and CAT-E. If the activity of the two catalysts was re-written per surface area unity, the combustion profile showed by CAT-I was always higher than that of CAT-E. This behaviour underlines the occurrence of intrinsic differences between the two catalysts which are responsible for their different catalytic activity.

The two catalysts were subjected to durability tests collecting, after the first run performed on fresh samples, three other runs in the temperature range 550–650°C, which corresponded to 20–90% of CH_4 conversion. The tests were performed at various contact times chosen in the interval 0.047–0.315 s. As a general trend, the massive catalyst showed higher stability than the supported one. Figures 2 and 3 report the results obtained for runs performed at contact times of 0.153 and 0.159 s for CAT-E and CAT-I, respectively. The data of activity of CAT-E at each temperature were spread in the range ±1–3% for the four runs. It could not be observed a clear deactivation of CAT-E passing from the 1st to the 4th run (figure 2). Inversely, CAT-I showed a detectable progressive decrease of activity, that could be estimated

Table 3
Surface elemental composition of the catalysts determined by XPS analysis

Element	CAT-E				CAT-I			
	atomic (%)	binding energy (eV)	oxidation state	atomic ratio	atomic (%)	binding energy (eV)	oxidation state	atomic ratio
Ba ($3d_{5/2}$)	0.4	780.70	II		0.6	780.40	II	
Cr ($2p_{3/2}$)	7.8	575.90 578.95	III (70%) VI (30%)	$Cr^{VI}/Cr^{III} = 0.4$	2.7	576.49 579.45	III (77%) VI (23%)	$Cr^{VI}/Cr^{III} = 0.3$
Cu ($2p_{3/2}$)	2.4	931.22 933.97	I (8%) II (92%)	$Cu^{II}/Cu^{I} = 12$	2.8	932.31 934.55	I (42%) II (58%)	$Cu^{II}/Cu^{I} = 1.4$
O (1s)	77	531.71 530.08	(19%) (81%)		53	532.29 530.52	(11%) (89%)	
Al (2p)					32	118.60	III	
C (1s)	12	284.60			8.2	284.60		

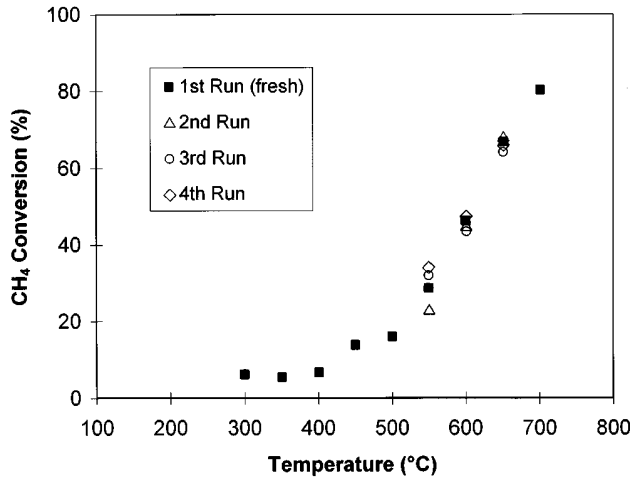

Figure 2. Durability test over CAT-E obtained through discontinuous experiments as a function of temperature ($\tau = 0.153$ s; CH_4 : air = 1 : 30; $p_{CH_4} = 0.012$ atm).

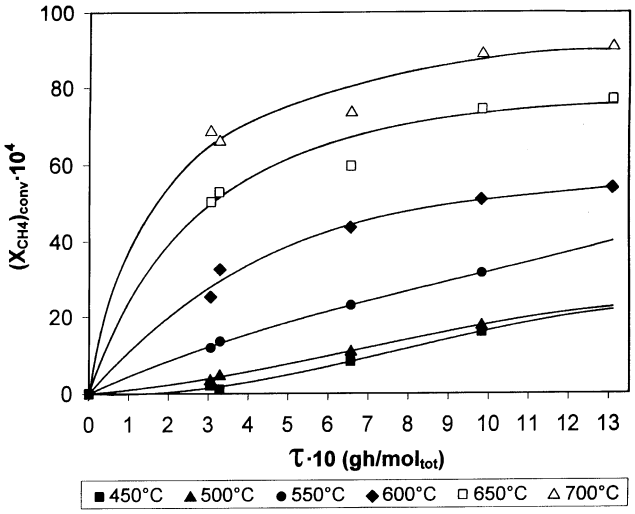

Figure 4. Molar fraction of converted methane ($(X_{CH_4})_{conv}$) over CAT-E as a function of contact time (τ) at different temperatures.

on an average of 15–20% of lowering of CH_4 conversion (figure 3). In conclusion, CAT-I possessed higher catalytic activity than CAT-E for methane combustion, but CAT-E showed better stability.

3.3. Kinetic analysis

The difference in catalytic activity between the massive copper chromite and the supported one was deeper investigated performing a kinetic analysis. Combustion profiles of methane were collected on each catalyst in the temperature range between 450 and 700°C as a function of contact time at constant CH_4 : air ratio. Fresh samples of the catalysts were used for each run at a given contact time in order to prevent the collection of data affected by catalyst deactivation. Values of τ were chosen in the range 0.047–0.211 s and in the range 0.047–0.159 s for CAT-E and CAT-I, respectively. The operative conditions utilized corresponded to CH_4 conversion in the interval 0–20% for the two catalysts at the lowest temperature (450°C), and between 50 and 80% and between 80 and 90% for CAT-E and CAT-I, respectively, at the highest temperature (700°C).

Figures 4 and 5 present the results obtained in terms of converted methane molar fraction, $(X_{CH_4})_{conv}$, versus contact time (τ, expressed as ratio of the catalyst weight to the total molar flow of feed). The curves of figures 4 and 5 show regular increasing trends until the attainment of a more or less marked plateau. The values of $(X_{CH_4})_{conv}$ for a given value of τ increased with temperature, as expected due to the activation of the reaction by temperature.

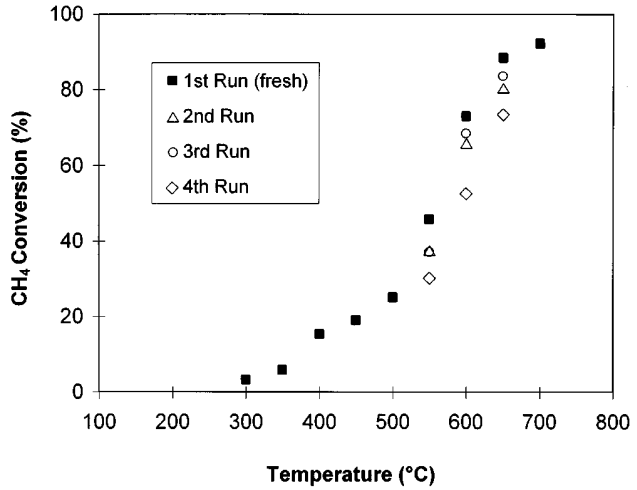

Figure 3. Durability test over CAT-I obtained through discontinuous experiments as a function of temperature ($\tau = 0.159$ s; CH_4 : air = 1 : 30; $p_{CH_4} = 0.012$ atm).

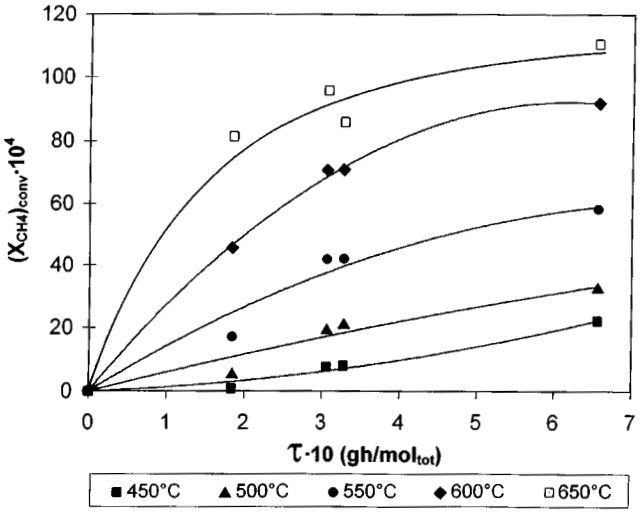

Figure 5. Molar fraction of converted methane ($(X_{CH_4})_{conv}$) over CAT-I as a function of contact time (τ) at different temperatures.

The derivative of the points reported in figures 4 and 5 could directly provide the values of reaction rate (r). Then, the experimental points relevant to each reaction temperature were interpolated by polynomial equations. The derivative of these equations with respect to contact time allowed the values of reaction rate to be calculated. The values of r were calculated at given values of molar fraction of converted methane, and they are presented in tables 4 and 5 for different temperatures at each X_{CH_4} converted. It can be seen that the reaction rates were between 10^{-3} and 10^{-4} $mol_{CH_4}/(g\ h)$ for both the catalysts. As expected the values showed an increasing trend as temperature increased. The values of reaction rate as a function of contact time at each reaction temperature followed a decreasing pseudo-exponential trend for CAT-E, and a quite linear decreasing trend for CAT-I. This behaviour suggested the occurrence of different reaction orders for the combustion reaction with respect to methane over the two catalysts.

In order to evaluate the dependence of the reaction rates on temperature, the curves collected at temperatures between 550 and 700°C for CAT-E and between 550 and 650°C for CAT-I and the relevant reaction rates reported in the tables 4 and 5 were considered. The values of the activation energy (E_a) for the two catalysts were then calculated through Arrhenius equation. Figures 6 and 7 report the relations $\ln(r)$ vs. $1/T$ for different degrees of the molar fraction of converted methane, for both the catalysts. In any case, very close slopes of the Arrhenius lines were obtained for different values of $(X_{CH_4})_{conv}$. On this basis, a mean Arrhenius line was calculated for each catalyst. The slope of the mean Arrhenius line gave the value of E_a. Values of 105.99 ± 10.4 kJ/mol and 118.21 ± 0.6 kJ/mol were computed for CAT-E and CAT-I, respectively. It can be observed that for both the catalysts the obtained activation energies were in the same region of values considering their relevant reliability interval.

Table 4
Reaction rate for CH_4 combustion over CAT-E evaluated at different temperatures and converted methane molar fraction ($(X_{CH_4})_{conv}$)

$(X_{CH_4})_{conv} \times 10^4$	T (°C)	$\tau \times 10$ (s)	$\tau \times 10$ ((g h)/mol_{tot})	$r \times 10^4$ ($(mol_{CH_4})_{conv}$/(g h))
25	550	1.13	7.33	2.41
	600	0.41	2.65	3.62
	650	0.19	1.26	16.20
	700	0.14	0.88	23.70
28	550	1.30	8.45	2.08
	600	0.47	3.06	6.79
	650	0.22	1.44	15.50
	700	0.15	1.00	30.00
31	550	1.50	9.60	2.52
	600	0.54	3.50	6.21
	650	0.25	1.63	14.70
	700	0.17	1.13	22.20
36	550	1.77	11.50	2.61
	600	0.67	4.36	5.15
	650	0.31	1.98	13.40
	700	0.21	1.36	20.80

Table 5
Reaction rate for CH_4 combustion over CAT-I evaluated at different temperatures and converted methane molar fraction ($(X_{CH_4})_{conv}$)

$(X_{CH_4})_{conv} \times 10^4$	T (°C)	$\tau \times 10$ (s)	$\tau \times 10$ ((g h)/mol_{tot})	$r \times 10^4$ ($(mol_{CH_4})_{conv}$/(g h))
35	550	0.66	2.73	5.58
	600	0.31	1.30	27.00
	650	0.19	0.79	35.20
37	550	0.66	3.00	5.44
	600	0.34	1.42	23.10
	650	0.21	0.87	34.60
39	550	0.77	3.20	5.34
	600	0.36	1.50	22.70
	650	0.22	0.92	34.20
42	550	0.84	3.50	5.19
	600	0.39	1.62	22.10
	650	0.24	1.00	33.60

4. Conclusions

The two investigated catalysts had a similar elemental composition and they differed in the alumina content, alumina played the role of binder or support in CAT-E and CAT-I, respectively. The different behaviour of CAT-I towards the total combustion of methane was probably related to the presence of particular active

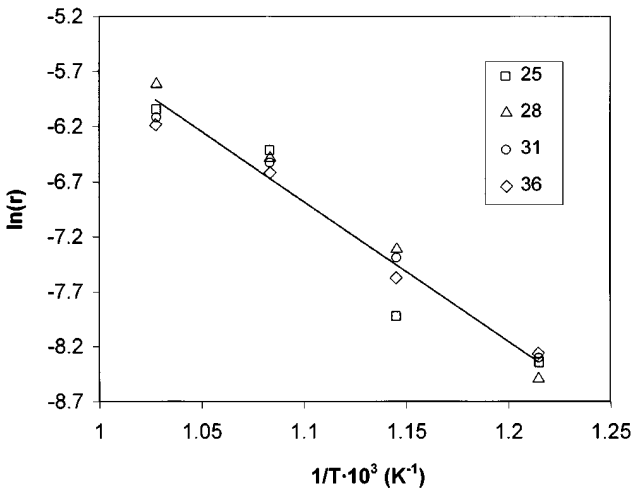

Figure 6. Arrhenius plot for the combustion of methane over CAT-E at different molar fraction of converted methane ($(X_{CH_4})_{conv}$); r is expressed in $(mol_{CH_4})_{conv}/(g\ h)$.

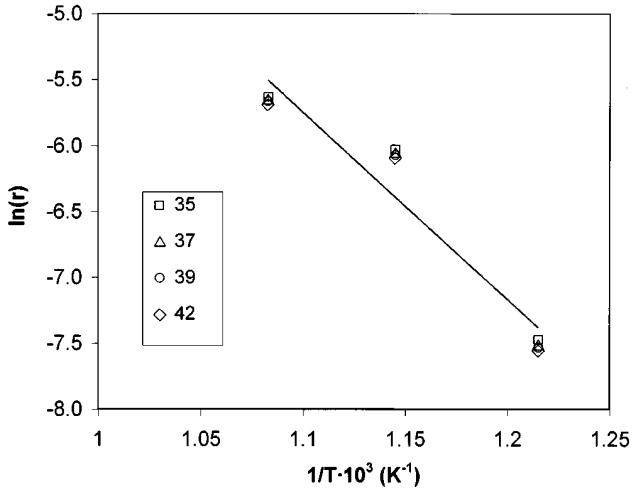

Figure 7. Arrhenius plot for the combustion of methane over CAT-I at different molar fraction of converted methane ($(X_{CH_4})_{conv}$); r is expressed in $(mol_{CH_4})_{conv}/(g\,h)$.

phases dispersed on the support. In fact, different crystalline phases were stabilized in the two catalysts, as detected by XRD analyses.

The massive catalyst, CAT-E, showed a higher chromium amount on the surface, while the Cr^{VI}/Cr^{III} surface ratio remained quite the same passing from CAT-E to CAT-I. As regards surface copper content, it was similar for both the catalysts. The surface Cu^{II}/Cu^{I} ratio deeply differed between the two catalysts, it was about unity on the CAT-I surface while great predominance of Cu^{II} was present on the CAT-E surface. It is well-known that the activity of mixed metal oxides depends on the presence of redox couples on the catalyst surface [1,9]. In fact, the catalytic mechanism of methane oxidation is based on the adsorption of oxygen on active sites, which alternatively pass from a reduced to an oxidized form, following a Rideal–Eley or a Langmuir–Hinshelwood model [3]. Thus, the higher activity of CAT-I could be due to the presence of the Cu^{II}/Cu^{I} couple which could work in synergic way with the Cr^{VI}/Cr^{III} couple, present in both the catalysts.

As regards stability, it can be observed that the lower amount of active components loaded on the supported catalyst made CAT-I more unstable than CAT-E. In fact, the massive catalyst showed an excellent stability which was probably due to the presence of high amount of the mixed crystalline phase containing both copper and chromium ($CuCr_2O_4$).

As known from literature [9], oxides containing Co, Cr, Mn, Fe, Cu, and Ni are potentially interesting for catalytic combustion. As expected, the copper chromite studied in this work can offer interesting performances in view of application. Detailed comparisons with other oxide catalysts of different studies is difficult because of the differences in test conditions and methods used to interpret the kinetic data. It seems more interesting to compare the catalytic activity of CAT-E and CAT-I with noble metal catalysts. In this perspective a Pd/Al_2O_3 catalyst has been chosen [27]. It was observed that the light-off temperature was about 150–200°C lower for Pd/Al_2O_3 than for CAT-E and CAT-I. Moreover, methane conversion was already complete at 475°C for Pd/Al_2O_3. A value of E_a of about 90 kJ/mol [27] was found for Pd/Al_2O_3 which was comparable with the average value of about 110 kJ/mol obtained for the copper chromite oxides.

When noble metal catalysts are employed for combustion, it is preferable to use low temperature to avoid sintering and deactivation problems to prolong the catalyst life. In this case, a secondary catalytic unit for completing the combustion is generally expected. The most interesting appliances of mixed oxide catalysts could be as secondary catalytic combustor after a first catalytic unit had performed the reaction ignition. The results presented confirm the possibility of interesting appliances of mixed metal oxides for high temperature catalytic combustion.

Acknowledgement

The authors wish to thank Dr. L. Tsikoza (Boreskov Institute of Catalysis, Novosibirsk) for the preparation of catalyst. The authors are also indebted to Engelhard Italy, and in particular to Dr. C. Cavenaghi for supplying the catalyst.

References

[1] R. Prasad, L.A. Kennedy and E. Ruckenstein, Catal. Rev. Sci. Eng. 26 (1984) 1.
[2] L.D. Pfefferle and W.C. Pfefferle, Catal. Rev. Sci. Eng. 29 (1987) 219.
[3] H. Arai and M. Machida, Catal. Today 10 (1991) 81.
[4] D.L. Trimm, Appl. Catal. 7 (1983) 249.
[5] H. Bosch and F. Janssen, Catal. Today 2 (1987) 369.
[6] H. Arai and H. Fukuzawa, Catal. Today 26 (1995) 217.
[7] K. Eguchi and H. Arai, Catal. Today 29 (1996) 379.
[8] J.J. Spivey, Ind. Eng. Chem. Res. 26 (1987) 2165.
[9] M.F.M. Zwinkels, S.G. Järås, P.G. Menon and T.A. Griffin, Catal. Rev. Sci. Eng. 35 (1993) 319.
[10] D.L. Trimm, Catal. Today 26 (1995) 231.
[11] R. Burch and P.K. Loader, Appl. Catal. B 5 (1994) 149.
[12] R. Burch and P.K. Loader, Appl. Catal. A 122 (1995) 169.
[13] R. Burch and F.J. Urbano, Appl. Catal. A 124 (1995) 121.
[14] R. Burch, F.J. Urbano and P.K. Loader, Appl. Catal. A 123 (1995) 173.
[15] J.G. McCarty, Catal. Today 26 (1995) 255.
[16] K. Muto, N. Katada and M. Niwa, Appl. Catal. A 134 (1996) 203.
[17] K. Sekizawa, K. Eguchi, H. Widjaja, M. Machida and H. Arai, Catal. Today 28 (1996) 245.
[18] H. Arai, T. Yamada, K. Eguchi and T. Seiyama, Appl. Catal. 26 (1986) 265.
[19] J.G. McCarty and H. Wise, Catal. Today 8 (1990) 231.
[20] G. Saracco, G. Scibilia, A. Iannibello and G. Baldi, Appl. Catal. B 8 (1996) 229.

[21] C.T. Au, H.Y. Wang and H.L. Wan, J. Catal. 158 (1996) 343.
[22] P. Ciambelli, La Chimica e l'Industria (March 1996) 175.
[23] R. Prasad, L.A. Kennedy and E. Ruckenstein, Combust. Sci. Technol. 27 (1982) 171.
[24] A. Gervasini, C.L. Bianchi and V. Ragaini, in: *Environmental Catalysis*, ACS Symp. Ser. 552, ed. J.N. Armor (ACS, Washington, 1994) ch. 29.
[25] A. Gervasini, G.C. Vezzoli and V. Ragaini, Catal. Today 29 (1996) 449.
[26] G. Horvath and K. Kawazoe, Chem. Eng. Japan 16 (1983) 470.
[27] J. Chaouki, C. Guy, C. Sapundzhiev, D. Kusohorsky and D. Klvana, Ind. Eng. Chem. Res. 33 (1994) 2957.